ERK1/2 activation is a therapeutic target in age-related macular degeneration

Sami Dridi[a,1], Yoshio Hirano[a,1], Valeria Tarallo[a], Younghee Kim[a], Benjamin J. Fowler[a,b], Balamurali K. Ambati[c,d], Sasha Bogdanovich[a], Vince A. Chiodo[e], William W. Hauswirth[e], Jennifer F. Kugel[f], James A. Goodrich[f], Steven L. Ponicsan[f], David R. Hinton[g], Mark E. Kleinman[a], Judit Z. Baffi[a], Bradley D. Gelfand[a], and Jayakrishna Ambati[a,b,2]

[a]Department of Ophthalmology and Visual Sciences and [b]Department of Physiology, University of Kentucky, Lexington, KY 40506; [c]Department of Ophthalmology and Visual Sciences, Moran Eye Center, University of Utah School of Medicine, Salt Lake City, UT 84132; [d]Department of Ophthalmology, Veterans Affairs Salt Lake City Healthcare System, Salt Lake City, UT 84148; [e]Department of Ophthalmology, University of Florida, Gainesville, FL 32610; [f]Department of Chemistry and Biochemistry, University of Colorado, Boulder, CO 80309; and [g]The Arnold and Mabel Beckman Macular Research Center at the Doheny Eye Institute, University of Southern California, Los Angeles, CA 90033

Edited* by Napoleone Ferrara, Genentech, Inc., South San Francisco, CA, and approved July 10, 2012 (received for review April 18, 2012)

Deficient expression of the RNase III DICER1, which leads to the accumulation of cytotoxic Alu RNA, has been implicated in degeneration of the retinal pigmented epithelium (RPE) in geographic atrophy (GA), a late stage of age-related macular degeneration that causes blindness in millions of people worldwide. Here we show increased extracellular-signal-regulated kinase (ERK) 1/2 phosphorylation in the RPE of human eyes with GA and that RPE degeneration in mouse eyes and in human cell culture induced by DICER1 depletion or Alu RNA exposure is mediated via ERK1/2 signaling. Alu RNA overexpression or DICER1 knockdown increases ERK1/2 phosphorylation in the RPE in mice and in human cell culture. Alu RNA-induced RPE degeneration in mice is rescued by intravitreous administration of PD98059, an inhibitor of the ERK1/2-activating kinase MEK1, but not by inhibitors of other MAP kinases such as p38 or JNK. These findings reveal a previously unrecognized function of ERK1/2 in the pathogenesis of GA and provide a mechanistic basis for evaluation of ERK1/2 inhibition in treatment of this disease.

cell death | mobile elements | retinal degeneration

The *Alu* family of short interspersed elements (SINEs), the most abundant interspersed repeats in the human genome (1), has propagated to over 1 million copies via retrotransposition (2–4). These mobile elements have been considered selfish "junk DNA" entities in the host genome. However, it is now recognized that the RNAs transcribed from *Alu* and the related B1/B2 SINEs in rodents have complex regulatory functions such as transcriptional repression (5–7) and modulation of alternative splicing (8).

Although *Alu* polymorphisms confer significant genetic diversity to the human population (2), sporadic *Alu* insertions and *Alu*-mediated unequal recombination also cause a host of human genetic diseases (9). Indeed, *Alu*-mediated chromosomal disruption is involved in neurofibromatosis (10), hypercholesterolemia (11), and several cancers (12–14) via de novo insertion or recombination.

Recently, we identified *Alu* RNA as an enzymatic substrate for the RNase DICER1 (15) and showed that *Alu* RNA abundance is increased following DICER1 deficit in the retinal pigment epithelium (RPE) of human eyes with geographic atrophy (GA), the advanced non-neovascular form of age-related macular degeneration (AMD) that is characterized by RPE cell degeneration. *Alu* RNA accumulation following DICER1 deficiency induces human RPE cell death and RPE degeneration in mice via activation of caspase-1 and -3 and, remarkably, is also independent of miRNA and toll-like receptor pathways (15, 16). Still, the signaling mediators of *Alu* RNA cytotoxicity remain to be fully defined. We tested the hypothesis that mitogen-activated protein kinases (MAPK) might be involved in *Alu*-induced cell death, as MAPK protein phosphorylation is a prerequisite for many signal transduction pathways and, in particular, cell death (17). Here we identify activation of extracellular-signal-regulated kinase (ERK) 1/2—the "classical MAPKs"—as key mediators of DICER1 dysregulation or *Alu* RNA accumulation-induced RPE cell death in GA.

Results

ERK1/2 Activation in Human GA RPE. The clinical and pathological hallmark of GA in human eyes is RPE degeneration (18). In the atrophic macular region in human GA eyes (Fig. 1*A*), there is marked disruption of the tight-junction associated protein zonula occludens-1 (ZO-1) and dysmorphology of the RPE cell monolayer (Fig. 1*B*). In this diseased macular RPE, we observed increased levels of ERK1/2 MAPK phosphorylation compared with non-AMD eyes (Fig. 1*C*). In contrast, there was no difference in the phosphorylation of p38 MAPK and JNK1/2 (Fig. 1*C*) or in the expression of total ERK1/2 in diseased vs. nondiseased RPE. DICER1 mRNA abundance and protein levels were significantly reduced in RPE of these GA eyes compared with control RPE (Fig. 1 *D* and *E*), confirming our earlier observations (15). Similarly, as we reported earlier (15), there was a dramatic increase in the abundance of *Alu* RNA in GA RPE compared with normal RPE (Fig. 1*F*).

DICER1 Knockdown Activates ERK1/2. We hypothesized that ERK1/2 activation in the RPE of GA tissue was a consequence of reduced DICER1 levels. *Dicer1* was knocked out in mouse RPE by subretinal administration of an adeno-associated viral vector (AAV) coding for Cre recombinase under the control of the RPE-specific BEST1 promoter (AAV1-BEST1-Cre) (19) in *Dicer1*$^{f/f}$ mice. As in our prior studies, this Dicer1 deficit induced RPE degeneration as visualized by fundus imaging or by immunofluorescent analysis of the spatial distribution of ZO-1 (Fig. 2*A*). In contrast, contralateral eyes treated with control AAV1-BEST1-GFP or wild-type mouse eyes injected with subretinal AAV1-BEST1-Cre did not exhibit RPE degeneration. We confirmed that *Dicer1* was knocked out in the RPE in vivo (Fig. S1*A*) and that this resulted in increased abundance of B1 and B2 RNAs (Fig. S1*B*), which are *Alu*-like SINE elements in mice. *Dicer1* knockout also specifically induced ERK1/2 phosphorylation in mouse RPE in vivo; p38 MAPK or JNK1/2 phosphorylation levels were unchanged (Fig. 2*B*).

Author contributions: S.D. and J.A. designed research; S.D., Y.H., V.T., Y.K., S.B., M.E.K., J.Z.B., and B.D.G. performed research; V.A.C., W.W.H., J.F.K., J.A.G., S.L.P., and D.R.H. contributed new reagents/analytic tools; S.D., Y.H., V.T., and Y.K. analyzed data; and S.D., B.J.F., B.K.A., B.D.G., and J.A. wrote the paper.

The authors declare no conflict of interest.

*This Direct Submission article had a prearranged editor.

[1]S.D. and Y.H. contributed equally to this work.

[2]To whom correspondence should be addressed. E-mail: jamba2@email.uky.edu.

This article contains supporting information online at www.pnas.org/lookup/suppl/doi:10.1073/pnas.1206494109/-/DCSupplemental.

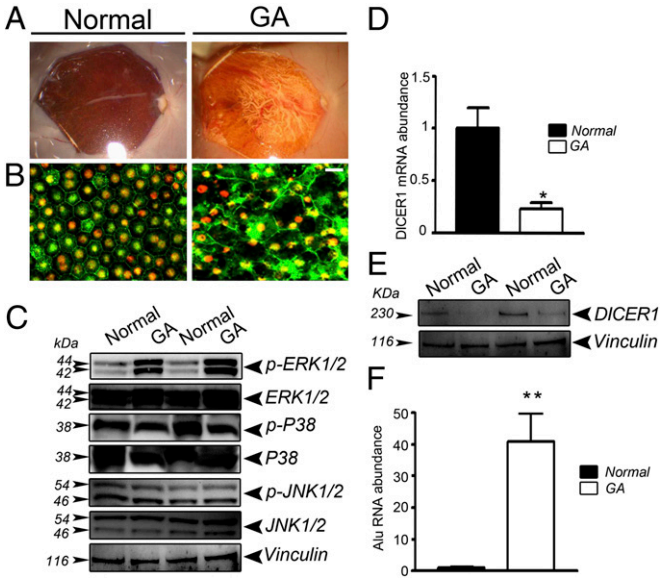

Fig. 1. DICER1 deficit in human GA RPE is accompanied by an increase in *Alu* RNA and ERK1/2 phosphorylation. (*A*) Fundus photographs and (*B*) flat mounts stained for ZO-1 (red) show cell degeneration and atrophy in RPE from a human GA eye compared with a normal eye. (Scale bar, 20 μm.) (*C*) ERK1/2 phosphorylation, assessed by Western blotting, is increased in human GA RPE compared with control RPE; however, p-p38 MAPK and p-JNK1/2 remained unchanged between the two groups. DICER1 quantification, assessed by quantitative PCR (*D*) and Western blotting (*E*), is lower in human GA RPE compared with control RPE (n = 5 independent experiments, $*P$ = 0.012 by Student's t test). (*F*) *Alu* RNA abundance is increased in human GA RPE compared with control RPE (n = 5 independent experiments, $**P <$ 0.0001 by Student's t test). Images are representative of three independent experiments (*C* and *E*).

Consonant with this observation, we found that inhibition of Dicer1 by Ad-Cre administration in *Dicer1*$^{f/f}$ mouse RPE cells induced a marked increase in ERK1/2 phosphorylation (Fig. 2*C*) with no effect on p38 or JNK1/2 activation. Similarly, antisense oligonucleotide-mediated knockdown of DICER1 in primary human RPE cells increased phosphorylation of ERK1/2, but not of p38 or JNK1/2, as assessed by Western blotting and immunofluorescence analysis (Fig. 2 *D* and *E*). Collectively, these data demonstrate that loss of DICER1 promotes activation of ERK1/2.

***Alu*/B1/B2 RNA Induces ERK1/2 Activation.** Having previously identified *Alu* RNA as an enzymatic substrate of DICER1 cleavage and as abundant in GA RPE (15), we next tested whether *Alu*/B1/B2 RNA similarly triggers ERK1/2 activation. Subretinal injection of plasmids coding for *Alu* RNA (pAlu) or for B1 or B2 RNAs induced RPE degeneration (Fig. 3 *A* and *B*) and ERK1/2 phosphorylation (Fig. 3 *C* and *D*) in wild-type mice. *Alu* promoted specific phosphorylation of the ERK1/2 MAPK family, but not of two other MAPK families, because pAlu did not increase p38 MAPK or JNK1/2 phosphorylation in wild-type mouse RPE in vivo (Fig. 3*C*) or in cell culture (Fig. 3*E*). Consistent with this finding, both pAlu and in vitro-transcribed *Alu* RNA induced robust ERK1/2 phosphorylation in human RPE cells without affecting p38 or JNK1/2 activity (Fig. 3 *F* and *G*). Plasmids encoding B1 and B2 expression increased ERK1/2 activation in wild-type mouse RPE in vivo and in cell culture, indicating conservation of this effect in the related mouse repetitive element transcripts (Fig. 3 *D* and *H*). Together, these data confirm that *Alu* RNA specifically promotes ERK1/2 activation.

ERK1/2 Mediates DICER1 Deficit-Induced RPE Degeneration. We previously established that loss of DICER1 promotes RPE cell death (15, 16). Having determined that DICER1 deficit also induces ERK1/2 signaling in RPE, we tested whether ERK1/2 activation was necessary for RPE degeneration. Indeed, RPE degeneration in *Dicer1*$^{f/f}$ mice, induced by AAV-BEST1-Cre, was rescued by intravitreous administration of the MAPKK (MEK1) inhibitor PD98059, which blocks ERK phosphorylation, but not by inhibitors of p38 MAPK (SB202190) or JNK (SP600125) (Fig. 4*A*). Similarly, PD98059 also protected against human and wild-type mouse RPE cytotoxicity induced by DICER1 depletion (Fig. 4 *B* and *C*). In contrast, the p38 MAPK and JNK inhibitors did not rescue human or mouse RPE cell viability. We confirmed the mechanism of action of PD98059 by finding that it blocked ERK1/2 activation induced by DICER1 knockdown in human or wild-type mouse RPE cells (Fig. 4 D–F). Furthermore, subretinal

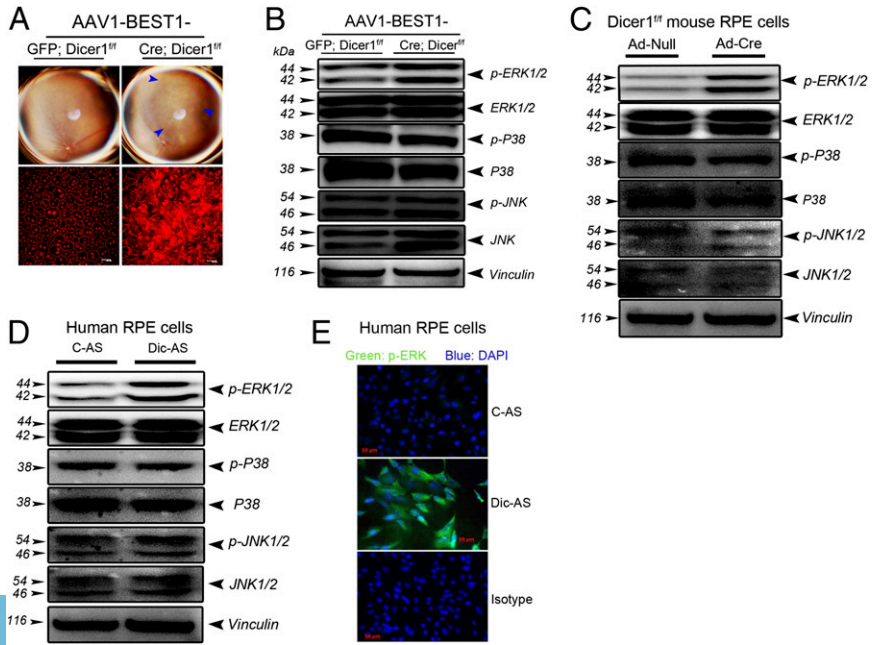

Fig. 2. DICER1 knockdown induces B1/B2 (*Alu*-like) RNA accumulation, RPE cell death, and ERK1/2 phosphorylation. (*A*) Fundus photographs and flat mounts stained for ZO-1 (in red) show RPE degeneration in *Dicer1*$^{f/f}$ mice following subretinal injection of AAV1-BEST1-Cre but not AAV1-BEST1-GFP. (*B*) Subretinal administration of AAV1-BEST1-Cre in *Dicer1*$^{f/f}$ mice induces ERK1/2 phosphorylation in the RPE compared with AAV1-BEST1-GFP. (*C*) Ad-Cre infection of RPE cells isolated from *Dicer1*$^{f/f}$ mice promotes activation of ERK1/2 but not p38 MAPK or JNK1/2 compared with Ad-Null. DICER1 antisense (Dic-AS) increases ERK1/2 phosphorylation but not p-p38 MAPK or p-JNK1/2 in human RPE cells assessed by Western blotting (*D*) and immunofluorescence (*E*). Images are representative of three to four independent experiments (*A*–*E*).

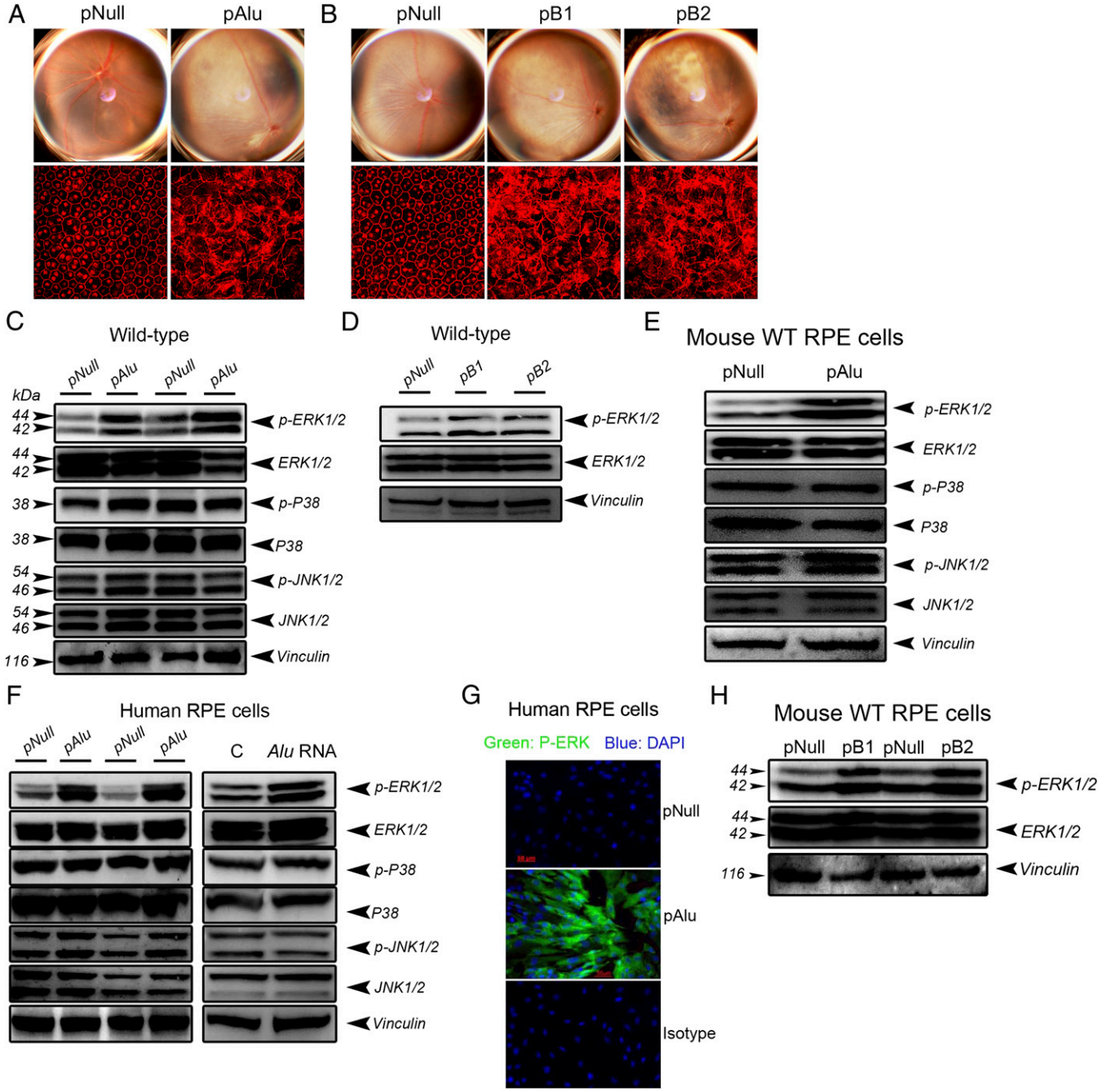

Fig. 3. *Alu*/B1/B2 overexpression or *Alu* RNA induces RPE degeneration and activates ERK1/2. (*A* and *B*) Fundus photographs and flat mounts stained for ZO-1 (in red) show RPE degeneration in wild-type mice following subretinal transfection of pAlu (*A*) and pB1 and pB2 (*B*). (*C* and *D*) Subretinal transfection of plasmids coding for *Alu* (*C*) or B1 or B2 RNA increases ERK1/2 phosphorylation in the RPE of wild-type mice (*D*). Overexpression of *Alu* or B1 or B2 promotes ERK1/2 activation in wild-type mouse RPE cells (*E* and *H*) and human RPE cells (*F* and *G*). (*C*–*F* and *H*) Western blotting. (*G*) Immunofluorescence. Images are representative of three to four independent experiments (*A*–*H*).

delivery of a plasmid coding for full-length MAPKKK (MEK1), which activates ERK1/2 (20), induced RPE degeneration in wild-type mice (Fig. 4*G*), supporting the concept that ERK1/2 activation is sufficient to induce RPE degeneration. Collectively, these data identify ERK1/2 as an essential component of DICER1 deficit-induced RPE degeneration.

ERK1/2 Mediate *Alu*/B1/B2-Induced RPE Degeneration. We evaluated whether *Alu*, B1, and B2 RNAs require ERK1/2 activation to promote RPE degeneration. The MEK inhibitor PD98059 prevented RPE degeneration induced by *Alu* RNA (Fig. 5*A*) or B1/B2 RNA in wild-type mice (Fig. 5*B*). In contrast, p38 or JNK1/2 inhibitors did not confer protection against *Alu*-induced RPE degeneration even when used at concentrations supramolar to the ERK inhibitor (Fig. 5*A* and Fig. S2*A*). Similarly, treatment of primary human or wild-type mouse RPE cells with PD98059, but not with p38 or JNK1/2 inhibitors, prevented pAlu-induced cell death (Fig. 5 *C* and *D*). We confirmed that PD98059, but not SB202190 or SP600125, reduced pAlu-induced ERK1/2 phosphorylation in both human and wild-type mouse RPE cells (Fig.

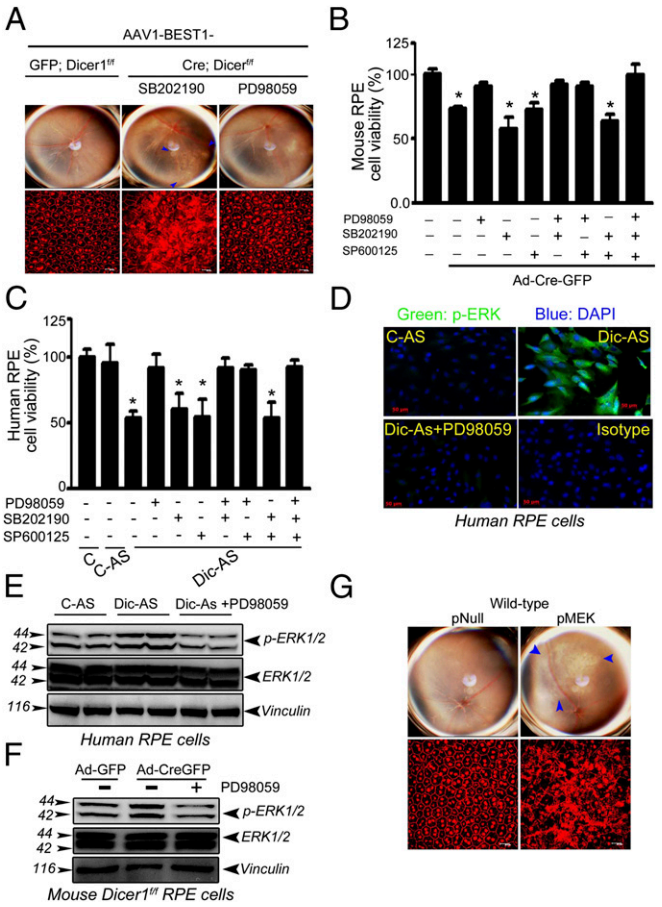

Fig. 4. ERK1/2 inhibition rescues mouse RPE cell death induced by DICER1 knockdown. (*A*) The ERK1/2 inhibitor PD98059, but not p38 (SB202190) or JNK inhibitor (SP600125), protects the RPE of *Dicer1*$^{f/f}$ mice from Dicer1 knockdown-induced degeneration after AAV1-BEST1-Cre administration. PD98059, but not SB202190 (p38 MAPK inhibitor) or SP600125 (JNK inhibitor), rescues viability of mouse (*B*) and human RPE cells (*C*) after DICER1 depletion. PD98059 inhibits Dicer1 knockdown-induced ERK1/2 activation in mouse and human RPE cells (*D–F*). Subretinal transfection of plasmid coding for full-length MAPKKK (MEK1) induces RPE degeneration in wild-type mouse (*G*). Values are mean ± SEM, $n = 3$ independent experiments, $^*P < 0.05$ by ANOVA and post hoc Newman–Keuls test (*B* and C). Images are representative of three to four independent experiments (*A* and *D–G*).

S2 *B–E*), confirming its mode of action. Together, these data reveal ERK1/2 activation as necessary for *Alu* RNA-mediated RPE degeneration.

***Alu* Accumulation Is Responsible for DICER1 Deficit-Induced ERK1/2 Activation.** Because DICER1 reduction not only can lead to the accumulation of *Alu* RNA but also can induce miRNA expression deficits, we sought to determine whether *Alu* RNA accumulation was responsible for DICER1 deficit-induced ERK1/2 activation. Indeed, both ERK1/2 phosphorylation and cell death induced by DICER1 depletion in human RPE cells were inhibited by antisense oligonucleotides targeting *Alu* RNA sequences, but not by scrambled antisense control (Fig. 6 *A–C*). These data indicate that DICER1 dysregulation promotes ERK1/2 activation via *Alu* RNA accumulation.

Discussion

In this study, we have extended our earlier observation that in human eyes with GA there is a deficiency of DICER1 and accumulation of *Alu* RNA in the RPE, and we also identified ERK1/2 activation as a signaling mediator of *Alu* RNA/DICER1 deficit-induced RPE degeneration. We found that there is increased activation of these MAP kinases in the RPE of human eyes with GA and that DICER1 loss or *Alu* RNA excess activates ERK1/2 in vivo. The critical nature of ERK1/2 activation in mediating RPE cytotoxicity in the context of DICER1/*Alu* RNA imbalance was demonstrated by rescuing RPE degeneration both in RPE cell culture and in mice via inhibition of ERK1/2.

We previously reported that RPE degeneration in DICER1-deficient or *Alu* RNA excess states is mediated by IL-18 derived from NLRP3 inflammasome activation (16). However, the ensuing signaling pathways that trigger RPE cell death are undefined. Our finding that RPE degeneration is mediated through ERK1/2 activation elucidates the cell death mechanisms downstream of IL-18 and is compatible with earlier observations that IL-18 can activate ERK1/2 (21).

Akin to the RPE, conditional ablation of *Dicer1* in the forebrain has been reported to induce ERK1 activation (22); however, the pathway linking these events remains to be resolved. Oxidative stress, which is postulated to be a key driver of AMD pathogenesis (23), is an attractive candidate. Previously, we have shown that hydrogen peroxide-induced oxidative stress down-regulates DICER1 (15) and that DICER1/*Alu* RNA

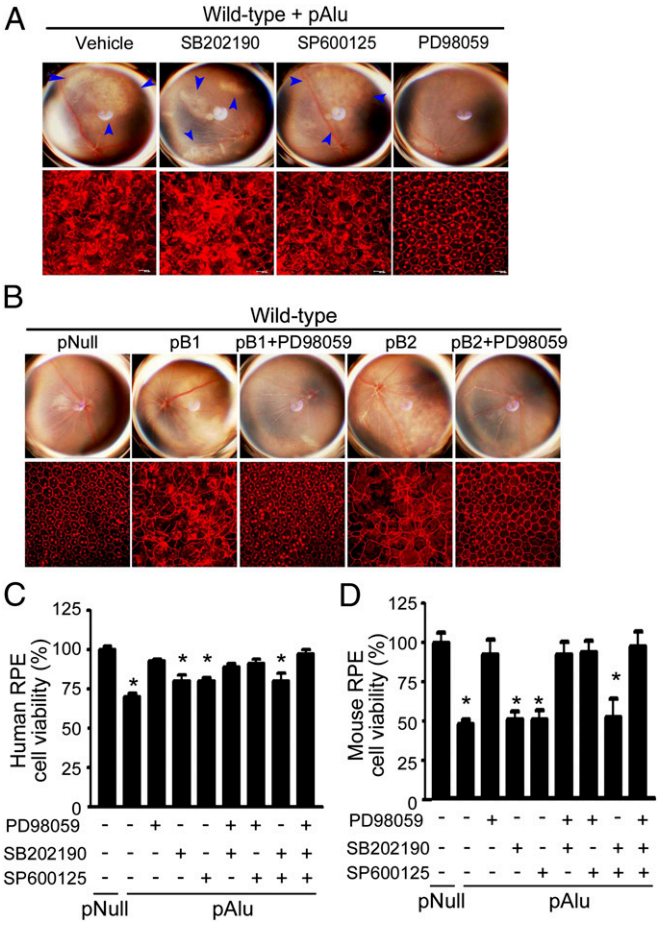

Fig. 5. ERK1/2 inhibition protects mouse and human RPE from *Alu*/B1/B2-induced cytotoxicity. PD98059, but not p38 (SB202190) or JNK inhibitor (SP600125), protects RPE cells from pAlu (*A*) or pB1/B2 cytotoxicity (*B*) in wild-type mice. PD98059 rescues human (*C*) and wild-type mouse RPE cell viability (*D*) after pAlu transfection. Values are mean ± SEM, $n = 3$, $^*P < 0.05$ by ANOVA and post hoc Newman–Keuls test. Images are representative of three to four independent experiments (*A–D*).

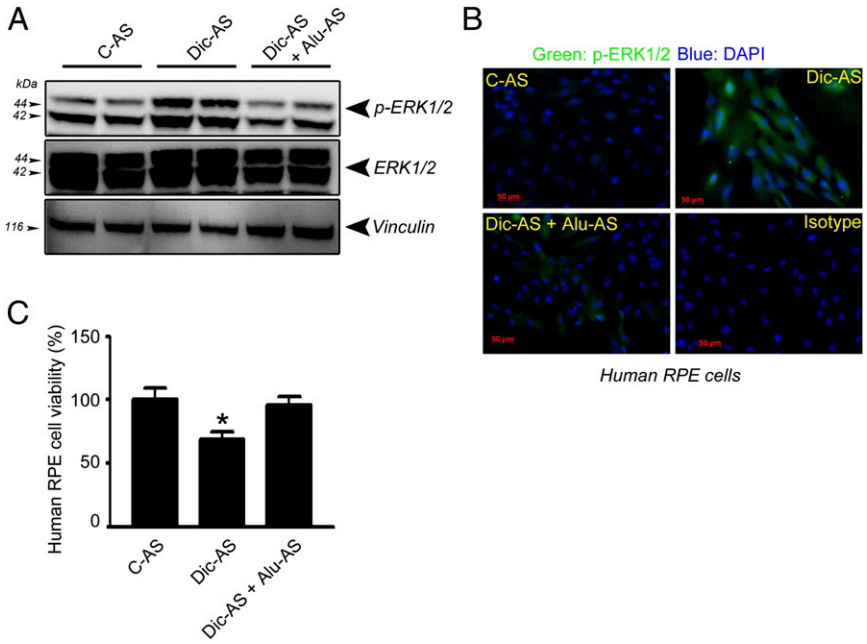

Fig. 6. *Alu* antisense inhibits ERK1/2 activation induced by DICER1 knockdown and rescue cell viability in human RPE cells. *Alu* antisense (Alu-AS) transfection inhibits ERK1/2 phosphorylation induced by DICER1 knockdown assessed by Western blotting (*A*) and immunofluorescence (*B*). *Alu*-AS protects human RPE cells from cytotoxicity induced by DICER1 knockdown (*C*). Values are mean ± SEM, $n = 3$, $^*P < 0.05$ by ANOVA and post hoc Newman–Keuls test. Images are representative of three independent experiments (*A*–*C*).

dysregulation induces mitochondrial ROS production in RPE cells (16). It is also known that chemically induced oxidative stress can trigger ERK1/2 activation in RPE cells (24). In addition, ERK1/2 activation can feed-forward to exacerbate oxidative stress (25).

As might be expected from the complexity of stress-related signaling pathways, ERK1/2 activation can promote both cell survival and apoptosis in a context-dependent manner (25, 26). One reason for these conflicting data might be the dichotomous response of ERK1/2 activation promoting cell survival in transient injury and cell death in chronic states (27). Consistent with this temporal dichotomy, ERK1/2 activation promotes cell death in a variety of chronic neurodegenerative states (27). Thus, our finding that ERK1/2 activation triggers RPE cell death in GA is compatible with the chronic nature of AMD progression.

Collectively, our findings—that there is increased activation of ERK1/2 in the RPE of human eyes with GA and that ERK1/2 inhibition blocks RPE degeneration in an in vivo model that recapitulates the DICER1/*Alu* RNA imbalance existing in the human disease state—provide a molecular rationale for exploring ERK1/2 inhibition strategies in atrophic AMD. In addition, ERK1/2 pathways also regulate angiogenesis and are involved in experimental models of retinal and choroidal neovascularization (28, 29). Thus, ERK1/2 activation also is a potentially attractive dual target for both atrophic and neovascular AMD. However, given the contextual roles of ERK1/2 activation in cell survival and death, pharmacological modulation of this signaling pathway is likely to demand careful optimization.

Materials and Methods

Descriptions of the following are available in *SI Materials and Methods*: Plasmids, mouse and human primary RPE cell isolation, culture and treatment, viral vectors, real-time PCR, antibodies, reagents, RNA isolation, immunolabeling, and protein quantification.

Animals. C57BL/6J and *Dicer1*$^{f/f}$ mice were purchased from The Jackson Laboratory. Ablation of *Dicer1* in these mice was accomplished using adeno-associated virus vector coding for Cre recombinase under control of an RPE-specific promoter.

Subretinal Injection. Transfection of plasmids using 10% (vol/vol) Neuroporter (Genlantis) was achieved by subretinal injections (1 μL) in mice using a Pico-Injector (PLI-100; Harvard Apparatus).

Drug Injections. Inhibitors of MEK1, p38 MAPK, and JNK were administered by intravitreous injection using a 33-gauge double-caliber needle (Ito Corporation).

In Vitro Transcription of *Alu* RNA. *Alu* RNA was synthesized using the AmpliScribe T7-*Flash* Transcription Kit (Epicentre) according to the manufacturer's instructions.

Transfection and Viral Infection of Cell Culture. Human and mouse RPE cells were pretreated with inhibitors of MEK1, p38 MAPK, and JNK 30 min before transfection. Cells were transfected with plasmids or antisense oligonucleotides using Lipofectamine 2000 according to the manufacturer's instructions. Cells were infected with Ad-Cre-GFP or Ad-Null at multiplicity of infection of 1,000 (Vector Laboratories).

Cell Viability. Cell viability was performed using MTS assays (CellTiter 96 AQueous One Solution Cell Proliferation Assay) according to the manufacturer's instructions (Promega).

ACKNOWLEDGMENTS. We thank A. Brunet, J. Garcia-Perez, T. Heidmann, and J. V. Moran for providing reagents; R. King, L. Xu, M. McConnell, C. Payne, D. Robertson, G. Botzet, G. R. Pattison, and C. Spee for technical assistance; and A. M. Rao, G. S. Rao, and K. Ambati for discussions. J.A. was supported by National Eye Institute/National Institutes of Health (NIH) Grants R01EY018350, R01EY018836, R01EY020672, R01EY022238, R21EY019778, and RC1EY020442; a Doris Duke Distinguished Clinical Scientist Award; a Burroughs Wellcome Fund Clinical Scientist Award in Translational Research; the Dr. E. Vernon Smith and Eloise C. Smith Macular Degeneration Endowed Chair; and a Senior Scientist Investigator Award (Research to Prevent Blindness). The authors also acknowledge the following support: NIH Grant K08EY021521, the International Retinal Research Foundation, and the American Health Assistance Foundation (all to J.Z.B.); NIH Grant K08EY021757 (to M.E.K.); NIH Grants T32HL091812 and UL1RR033173 (to B.J.F., S.B., and M.E.K.); an Alcon Japan Research Award (to Y.H.); NIH Grant P30EY021721 and the Macula Vision Research Foundation (both W.W.H.); NIH Grants R01EY017182 and R01EY017950, a Veterans Administration Merit Award, and the Department of Defense (all to B.K.A.); NIH Grants

P30EY003040 and R01EY001545 (to D.R.H.); NIH Grant R01GM068414 (to J.F.K. and J.A.G.); departmental unrestricted grants from Research to Prevent Blindness (to J.A. and W.W.H.); and University of Kentucky Physician Scientist Awards (to J.Z.B. and M.E.K.).

1. Lander ES, et al.; International Human Genome Sequencing Consortium (2001) Initial sequencing and analysis of the human genome. *Nature* 409:860–921.
2. Batzer MA, Deininger PL (2002) Alu repeats and human genomic diversity. *Nat Rev Genet* 3:370–379.
3. Schmid CW, Jelinek WR (1982) The Alu family of dispersed repetitive sequences. *Science* 216:1065–1070.
4. Dewannieux M, Esnault C, Heidmann T (2003) LINE-mediated retrotransposition of marked Alu sequences. *Nat Genet* 35:41–48.
5. Mariner PD, et al. (2008) Human Alu RNA is a modular transacting repressor of mRNA transcription during heat shock. *Mol Cell* 29:499–509.
6. Allen TA, Von Kaenel S, Goodrich JA, Kugel JF (2004) The SINE-encoded mouse B2 RNA represses mRNA transcription in response to heat shock. *Nat Struct Mol Biol* 11: 816–821.
7. Espinoza CA, Allen TA, Hieb AR, Kugel JF, Goodrich JA (2004) B2 RNA binds directly to RNA polymerase II to repress transcript synthesis. *Nat Struct Mol Biol* 11:822–829.
8. Lev-Maor G, Sorek R, Shomron N, Ast G (2003) The birth of an alternatively spliced exon: 3′ splice-site selection in Alu exons. *Science* 300:1288–1291.
9. Deininger PL, Batzer MA (1999) Alu repeats and human disease. *Mol Genet Metab* 67: 183–193.
10. Wallace MR, et al. (1991) A de novo Alu insertion results in neurofibromatosis type 1. *Nature* 353:864–866.
11. Lehrman MA, Goldstein JL, Russell DW, Brown MS (1987) Duplication of seven exons in LDL receptor gene caused by Alu-Alu recombination in a subject with familial hypercholesterolemia. *Cell* 48:827–835.
12. Miki Y, Katagiri T, Kasumi F, Yoshimoto T, Nakamura Y (1996) Mutation analysis in the BRCA2 gene in primary breast cancers. *Nat Genet* 13:245–247.
13. Mauillon JL, et al. (1996) Identification of novel germline hMLH1 mutations including a 22 kb Alu-mediated deletion in patients with familial colorectal cancer. *Cancer Res* 56:5728–5733.
14. Strout MP, Marcucci G, Bloomfield CD, Caligiuri MA (1998) The partial tandem duplication of ALL1 (MLL) is consistently generated by Alu-mediated homologous recombination in acute myeloid leukemia. *Proc Natl Acad Sci USA* 95:2390–2395.
15. Kaneko H, et al. (2011) DICER1 deficit induces Alu RNA toxicity in age-related macular degeneration. *Nature* 471:325–330.
16. Tarallo V, et al. (2012) DICER1 loss and Alu RNA induce age-related macular degeneration via the NLRP3 inflammasome and MyD88. *Cell* 149:847–859.
17. Keshet Y, Seger R (2010) The MAP kinase signaling cascades: A system of hundreds of components regulates a diverse array of physiological functions. *Methods Mol Biol* 661:3–38.
18. Ambati J, Ambati BK, Yoo SH, Ianchulev S, Adamis AP (2003) Age-related macular degeneration: Etiology, pathogenesis, and therapeutic strategies. *Surv Ophthalmol* 48:257–293.
19. Alexander JJ, Hauswirth WW (2008) Adeno-associated viral vectors and the retina. *Adv Exp Med Biol* 613:121–128.
20. Pagès G, Brunet A, L'Allemain G, Pouysségur J (1994) Constitutive mutant and putative regulatory serine phosphorylation site of mammalian MAP kinase kinase (MEK1). *EMBO J* 13:3003–3010.
21. Kalina U, et al. (2000) IL-18 activates STAT3 in the natural killer cell line 92, augments cytotoxic activity, and mediates IFN-gamma production by the stress kinase p38 and by the extracellular regulated kinases p44erk-1 and p42erk-21. *J Immunol* 165: 1307–1313.
22. Hébert SS, et al. (2010) Genetic ablation of Dicer in adult forebrain neurons results in abnormal tau hyperphosphorylation and neurodegeneration. *Hum Mol Genet* 19: 3959–3969.
23. Ambati J, Fowler BJ (2012) Mechanisms of age-related macular degeneration. *Neuron* 75:26–39.
24. Glotin AL, et al. (2006) Sustained versus transient ERK1/2 signaling underlies the anti- and proapoptotic effects of oxidative stress in human RPE cells. *Invest Ophthalmol Vis Sci* 47:4614–4623.
25. Sawe N, Steinberg G, Zhao H (2008) Dual roles of the MAPK/ERK1/2 cell signaling pathway after stroke. *J Neurosci Res* 86:1659–1669.
26. Lu Z, Xu S (2006) ERK1/2 MAP kinases in cell survival and apoptosis. *IUBMB Life* 58: 621–631.
27. Subramaniam S, Unsicker K (2010) ERK and cell death: ERK1/2 in neuronal death. *FEBS J* 277:22–29.
28. Hua J, et al. (2011) Resveratrol inhibits pathologic retinal neovascularization in Vldlr (-/-) mice. *Invest Ophthalmol Vis Sci* 52:2809–2816.
29. Xie P, et al. (2011) Suppression and regression of choroidal neovascularization in mice by a novel CCR2 antagonist, INCB3344. *PLoS ONE* 6:e28933.